



Norwegian University of
Science and Technology

FE Simulation of the Fracture Behaviour of Alu-Steel Butt Welds Produced Using the Hybrid Metal Extrusion and Bonding (HYB) Process

TMM4560 - Engineering Design and Materials, Specialization Project

Project work fall 2019

By Audun A. S. Teige

Supervisor: Filippo Berto

Department of Mechanical and Industrial Engineering

Faculty of Engineering

Norwegian University of Science and Technology (NTNU), Trondheim

Abstract

Hybrid metal extrusion and bonding (HYB), is a solid-state bonding process that can make Al-Fe joints. Using conform extrusion, a filament material and a rotating pin. In this report an in-depth analysis of the existing FE-model on an Al-Fe joint, produced by HYB, discovers some needed improvements. However, the existing model seems to replicate the strength of the joint well in the case of large initial cracks or weld defects in the root.

A new FE-model for the third generation Al-Fe HYB-welds are presented. The joint is split in extrusion zone (EZ), heat affected zone (HAZ) as well as unaffected material. The new model is used to simulate the ductile fracture occurring in the third generation welds. The UTS from simulation differ from the results from the tensile test by about 4%. The fracture from simulation is also similar to the one from the tensile testing, occurring at an angle of approximately 30 degrees of the vertical axis in the HAZ and not in the EZ or Al-Fe interface. From this it is concluded that the model is a good starting point for further development of the model.

Sammendrag

Hybrid metal extrusion and bonding (HYB), er en fast fase sammenføynings prosess som kan produsere Al-Fe sveis. Ved bruk av conform ekstrudering, et tilsetningsmateriale og en roterende verktøytapp. Denne rapporten finner noen punkter som trenger forbedring på den eksisterende FE-modellen av Al-Fe sveiser produsert ved hjelp av HYB metoden. Men den eksisterende modellen gjenskaper styrken til sveisen bra ved store sprekker eller feil i sveiseroten.

En ny FE-modell for tredje generasjon Al-Fe HYB sveiser er presentert. Sveisen er delt inn i ekstruderings sone, varmepåvirket sone samt upåvirket materiale. Den nye modellen blir brukt til å simulere det duktile bruddet som skjer i tredje generasjons sveiser. Maksimal tøyespenning fra simuleringen avviker fra strekkprøve resultatene med 4%. Bruddet fra simulering er også likt det fra strekkprøvene, det skjer med en vinkel på omtrent 30 grader fra den vertikale aksens i den varmepåvirkede sonen og ikke i ekstruderings sonen eller i Al-Fe grenseflata. Fra dette er det konkludert at modellen er et godt startpunkt for videre utvikling av modellen.

Acknowledgement

I would like to express my gratitude to Professor Øystein Grong, founder of HyBond, and Lise Sandnes, PhD-candidate at NTNU, for all the help you have given me. I appreciate that you always make time for discussions and share your knowledge on the topic. A special thanks to Professor Øystein Grong for the time and effort spent on helping me with this report.

I would like to thank my supervisor Filippo Berto, Professor at NTNU. For giving me the opportunity to work on this project. Lastly, I want to thank the OPTIMALS research project for letting me participate in a project meeting and giving me feedback and input on this project.

Table of Contents

1	Introduction.....	1
1.1	Motivation	1
1.2	Objective	2
2	Theory	3
2.1	Aluminium.....	3
2.2	Steel.....	4
2.3	Methods used for welding aluminium to steel	5
2.3.1	Gas Metal Arc Welding	5
2.3.2	Cold Metal Transfer welding.....	6
2.3.3	Friction Stir Welding	7
2.4	Hybrid Metal Extrusion and Bonding (HYB)	7
2.4.1	First Generation Al-Fe HYB Welds	8
2.4.2	Second Generation Al-Fe HYB Welds	9
2.4.3	Third Generation Al-Fe HYB Welds	10
2.5	Finite element method (FEM)	11
2.6	In-Depth Review of the Second Generation FE-Model.....	11
2.6.1	Setup of the Model	11
2.6.2	Simulation Results.....	13
2.6.3	Needed Improvements.....	14
3	FE-Modelling of Third Generation Al-Fe HYB Weld	15
3.1	Setup of the Model	15
3.1.1	Partitioning of Different Zones	15
3.1.2	Materials Data	18
3.1.3	Simulation Results.....	21
4	Conclusion	24
4.1	Colcluding Remarks	24
4.2	Further work.....	24
5	Citations.....	25
6	Appendix.....	27
6.1	Appendix A.....	27

List of Figures

Figure 1 Development of the amount of primary and recycled Aluminium used globally (Soo et al. 2018)	1
Figure 2 Solubility of hydrogen in solid and liquid aluminium (The Lincon Electric Company 1994).....	4
Figure 3 Thermal conductivity of steel and aluminium (Masubuchi 2013)	5
Figure 4 Simple illustration of how the GMAW and CMT uses a torch and filler wire in the weld (Yang et al. 2013)	6
Figure 5 Illustration of FSW between Aluminium and steel (Wang et al. 2018)	7
Figure 6 Visualization of the pin placement and geometry for the first generation Al-Fe HYB-welds (Berto et al. 2018).....	8
Figure 7 Images of the weld with a red dotted line indicating the fracture path shown on (a) a broken tensile specimen (b) an intact tensile specimen. Showing how most of the fracture occurs in the aluminium (Berto et al. 2018)	8
Figure 8 Visualization of the pin placement and design for the second generation of HYB-weld (Mathiasson 2019)	9
Figure 9 Crack propagation during tensile test; (a) start of loading, (b) visible crack initiation, (c) final fracture (Mathiasson 2019).....	9
Figure 10 Visualization of pin placement in 3. generation HYB-welds (Grong, Sandnes, and Berto 2019a)	10
Figure 11 Strain development from tensile test. Results are visualised using DIC results, with strain going from 0 to 0.3 (Sandnes, L. Personal communication 2019)	10
Figure 12 Commonly used element families (Abaqus-manual 2010)	11
Figure 13 Illustration of the different sections in the FE model and materials assigned to them (Mathiasson 2019)	11
Figure 14 BSE micrographs at 100x magnification taken from the fracture-surface close to the weld root (Mathiasson 2019)	12
Figure 15 Mesh of the FE model; (a) in the thickness, (b) in the width of model (Mathiasson 2019).....	13
Figure 16 Plot showing the influence different initial cracks have on the fracture behaviour of the joint (Mathiasson 2019)	13
Figure 17 Strain in the simulation right before the final fracture for (a) a large initial crack of 0.8mm (b) a small initial crack of 0.03 mm (Mathiasson 2019).....	14
Figure 18 Preliminary partition of the different zones within the weld (Sandnes, L. Personal communication 2019)	15
Figure 19 Average hardness data taken at different points in the weld. 1, 0 and -1 on the left indicates hardness data taken 1mm over centre, in the centre and 1mm under centre of the weld thickness. (full table can be found in appendix A).....	16
Figure 20 Hardness data plot for 1mm over and 1mm under centre of the weld. Arrows indicating the HAZ placement.....	16
Figure 21 Illustration of the different sections in the FE model and materials assigned to them.....	17
Figure 22 Displacement and maximum force on the old FE model without a crack.....	18
Figure 23 Displacement and maximum force on the new model without a crack	18
Figure 24 Screenshots showing the placement of the virtual extensometer over the EZ (top) and HAZ (bottom) at (a) before loading without strain (b) after loading with strain	19
Figure 25 Engineering stress strain curve for HAZ and EZ obtained from DIC results	19

Figure 26 Stress-strain data for FM copied from SINTEF test done to the same FM on a previous occasion (SINTEF 2018).....	20
Figure 27 True stress plastic strain data for HAZ, EZ and FM.....	20
Figure 28 Mesh of the HAZ and EZ. With a red line indicating the interface between the sections.....	21
Figure 29 Reference point connected to surfaces on that are pinned in the tensile test used to apply boundary conditions and forced displacement	21
Figure 30 Reaction forces and displacement taken from the reference point where the forced displacement is applied.....	22
Figure 31 Equivalent plastic strain (PEEQ) development in the weld. From start of loading until right before fracture begins with a colour scale going from 0 to 0.3	22
Figure 32 Start of the fracture with a PEEQ scale from 0 to 0.5	23
Figure 33 Final fracture of the test specimen from simulation with a PEEQ scale from 0 to 0.5	23
Figure 34 Final fracture of the test specimen from tensile testing (Sandnes, L. Personal communication 2019)	23

List of Abbreviations

AM	Additive manufacturing
AS	Advancing side
BM	Base material
BSE	Backscattered electron
CMT	Cold metal transfer
DIC	Digital image correlation
EZ	Extrusion zone
FE	Finite element
FEM	Finite element method
FM	Filament metal
FSW	Friction stir welding
GMAW	Gas metal arch welding
HAZ	Heat affected zone
HYB	Hybrid metal extrusion and bonding
IMC	Intermetallic compound
PEEQ	Equivalent plastic strain
RS	Retreating side
UTS	Ultimate tensile strength

1 Introduction

1.1 Motivation

In recent times, climate change has been put on the agenda. Climate change is one of the biggest challenges we must overcome in the near future. Aluminium and other materials with high strength to weight ratio are going to play an important role in the fight against climate change. The aluminium production has increased drastically since the 1950s as can be seen from Figure 1. The development is expected to continue as aluminium is getting more and more application areas in addition be increasingly used in developed sectors (Soo et al. 2018). The automotive sector is seeing a significant increase in the use of aluminium because of the increased focus on emissions. To decrease emissions the automotive industry has worked on making engines more efficient, design optimization and reducing weight. To reduce the weight, the amount of aluminium in new vehicles are expected to increase by 40% from 2016 to 2028 (Drivealuminium 2017). Even with this increase, aluminium will not replace steel as the most used material in cars. Therefore, a good method which enables bonding between the metals will be important.

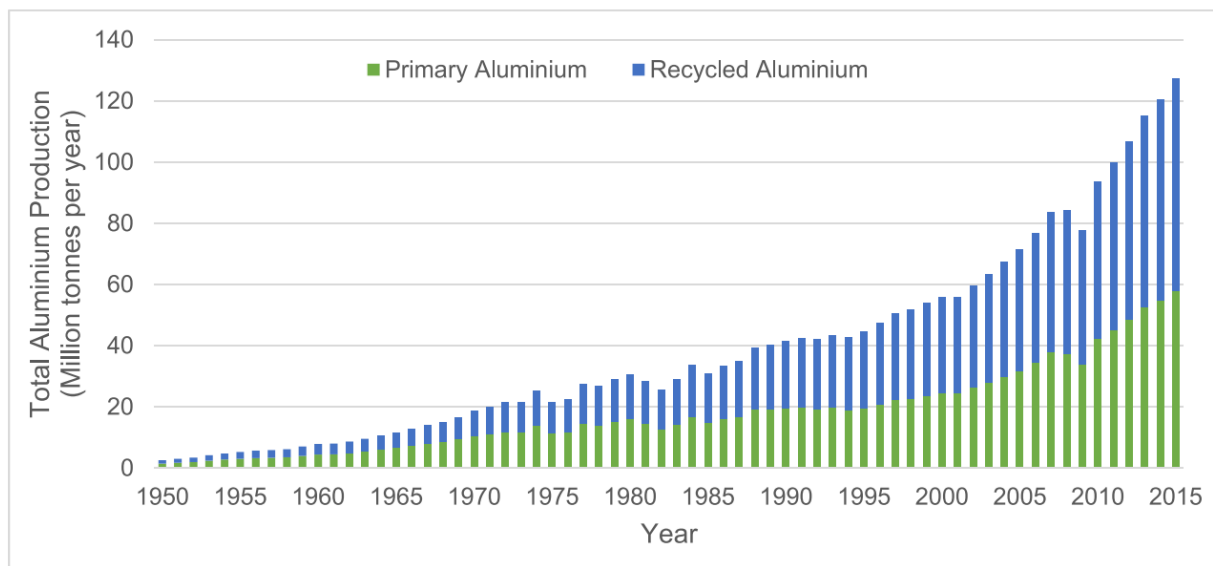


Figure 1 Development of the amount of primary and recycled Aluminium used globally (Soo et al. 2018)

Welding of aluminium and steel can be a challenging process. Many of the conventional methods of welding cannot be applied to aluminium-steel welds because of the large difference in properties. Some of the methods that have been successful in creating decent bonding between aluminium and steel are, Friction stir welding (FSW), Cold metal transfer (CMT), Gas metal arch welding (GMAW) and Hybrid metal extrusion and bonding (HYB) (Watanabe, Takayama, and Yanagisawa 2006) (Yang et al. 2013) (Shi et al. 2014) (Grong, Sandnes, and Berto 2019a). In particular, the solid-state joining methods like FSW and HYB have an advantage and focus on keeping the temperature down. Higher temperature increases the formation of intermetallic compound (IMC) between the aluminium and steel (Gullino, Matteis, and D'Aiuto (2019). IMC's are what bond the aluminium and steel

together and cannot be avoided. However, they show very low plastic deformability. Excessive formation of this IMC consequently makes the joint brittle. Thermal energy in the process will also create a larger heat affected zone (HAZ) that will have different physical properties than the base material. It is therefore concluded that reduction of heat absorbed by the aluminium is one of the main requirements for a good aluminium weld (Praveen and Yarlagadda 2005). This gives solid state bonding techniques like FSW and HYB an advantage.

Hybrid metal and extrusion bonding (HYB) is a new solid-state bonding method that uses continuous extrusion of a filament metal and rotation to form bonding. The process was developed for Al-Al butt welding. In recent years it has shown great promises in different applications, for example, in additive manufacturing (AM) and bonding of dissimilar metals (Blindheim, Welo, and Steinert 2019) (Grong, Sandnes, and Berto 2019b). Recent research and development of the Al-Fe bonding using HYB have shown great promise and this technique can be an important addition to the existing ones when it comes to production of dissimilar products in the future.

1.2 Objective

The main objectives of this project can be summarized in three points. The first one being a literature review. To see what the state of the art is, in joining of aluminium to steel. It is important to get a good understanding of the challenges this type of bonding is facing and see how the different welding methods work. This is important in order to put HYB in context and be able to compare it with other welding methods.

The second objective is to do an in-depth review and analysis of the existing FE-model for aluminium to steel joints made using second generation HYB welding. The model that will be reviewed is made by Marie Mathiasson in her master thesis in the spring of 2019 (Mathiasson 2019). By going through the existing model and focusing on areas that need improvement it will be easier to make an improved model for the next generation of aluminium-steel weld.

The third and largest objective of this project is to make an improved FE-model for aluminium-steel HYB joints in Abaqus. This new model will be used to analyse the third generation of HYB welds. The FE-model will be used to analyse the fracture behaviour and development in the weld. Much of the work will be new because of the development in the welding technique. However, something can be learned and re-used from the existing model. The goal for the new model is to be able to show results that are comparable with tensile test results. The idea is to continue working on this model in a master thesis in the spring of 2020.

2 Theory

2.1 Aluminium

Aluminium has a widespread use in the industry today because of material properties that gives the metal a wide range of applications. Aluminium is known as a lightweight metal with good corrosion resistance, high thermal and electrical conductivity and excellent formability (Lumley 2011). Aluminium is today widely used in the transportation and construction industries as well as in electrical products and consumer goods. Strength to weight ratio in aluminium is the most important attribute of the metal. This has given aluminium an important role in a lot of innovative products. From the construction of the empire state building to making airplanes. Aluminium is an essential material in the modern aircraft. Today the high strength to weight ratio is important to reduce the fuel consumption in the whole transportation industry and thereby reducing emissions. In construction and electrical industries, the low weight of aluminium reduces the need of support structures and foundations. In addition, the great corrosion resistance gives a natural protection against nature and reduces maintenance. Consumer goods have lately seen an increased use of aluminium. Electronic devices like laptops, phones and TVs are being made with more and more aluminium instead of plastic and steel. The high thermal conductivity can help reduce the heat of the component. However, the aluminium is mostly added for visual effects and to make the product appear durable and exclusive.

Pure aluminium has a low strength and are therefore often strengthened using different alloying elements. The alloys are categorized in different series based on their alloying elements. Alloys in the 6000 series, which this report will focus on, are used a lot in structural components. The main components of the alloys in the 6000 series are magnesium and silicon (Total materia 2003).

When welding aluminium the heat affected zone (HAZ) is one of the largest problems. This zone is normally softer and more ductile than the unaffected metal. This happens because of annealing processes that removes strain hardening and cold working in the material. Because of the high thermal conductivity in aluminium the HAZ becomes much wider in aluminium than in steel.

Because of the large difference in solubility of hydrogen between liquid and solid aluminium (Figure 2), gas porosity induced by hydrogen is another severe problem in fusion welding of aluminium. Excess hydrogen creates pores in the metal during solidification leading to reduced tensile and fatigue properties (Praveen and Yarlagadda 2005).

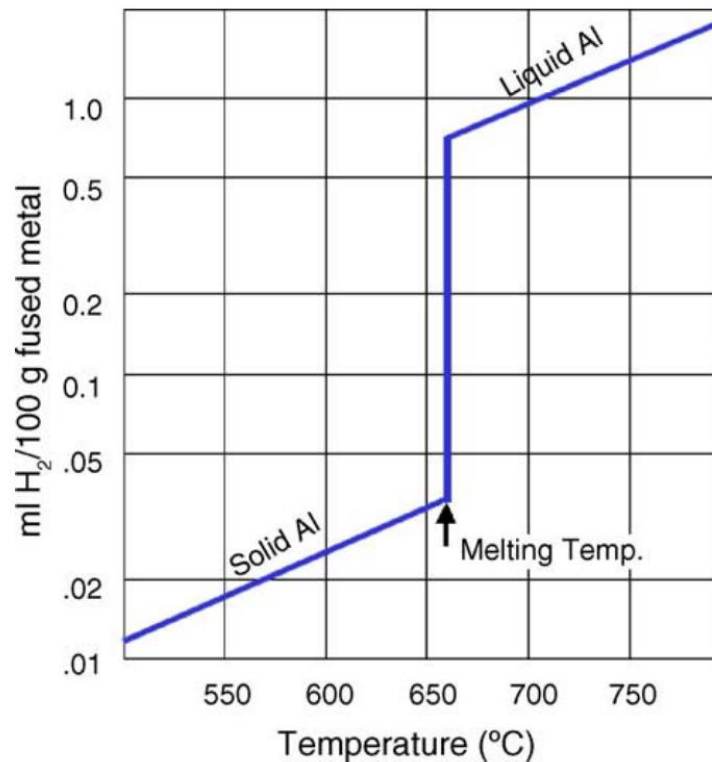


Figure 2 Solubility of hydrogen in solid and liquid aluminium (The Lincon Electric Company 1994)

2.2 Steel

Steel is the most widely used material today with over 1800 million tonnes produced in 2018 (Worldsteel 2019). Steel is used in almost every aspect of our life. From small everyday products to buildings and infrastructure. The widespread use of steel comes from the many areas of application for the metal. Steel has many areas of application because of the large range of properties, depending on treatment of the metal as well as alloying elements. Steel is around 2.5 times denser than aluminium but has a higher strength. However, aluminium's strength to weight ratio is higher than in steel. One other reason that steel is so widely used is that the cost of steel is relatively low compared with similar metals.

The most used steels are relatively easy to work with and work well in most applications as long as weight isn't a limiting factor. Most of the areas where other metals are used instead of steel are because of weight limitations or special characteristics. For example, corrosion resistance or biocompatibility.

Structural steel, as used in this Al-Fe weld, have many applications in a lot of different sectors. But mostly it's used in construction and transport. As previously mentioned, Al-Fe welds can be of great importance in transport to create bonding. When substituting steel with aluminium to reduce weight and fuel consumption.

2.3 Methods used for welding aluminium to steel

Welding of aluminium and steel is a challenging process but still necessary for some applications. As mentioned previously welding of aluminium can be a challenging process because of hydrogen porosity and HAZ softening. When joining aluminium and steel brittle intermetallic compounds (IMC's) must also be considered. Also, the large difference in thermal conductivity and thermal expansion are of importance (Figure 3). Because, it will create residual stresses and distortion in the welded material. All these challenges can be reduced in some way by decreasing the energy input in the weld. Therefore, reduction of heat input without compromising the bond strength is a common challenge for all Al-Fe welding methods. Tanaka et al. argued that IMC thickness largely affects the bond strength across the interface between aluminium and steel for FSW. This is because the bonding strength increases exponentially with decreasing IMC thickness (Tanaka, Morishige, and Hirata 2009).

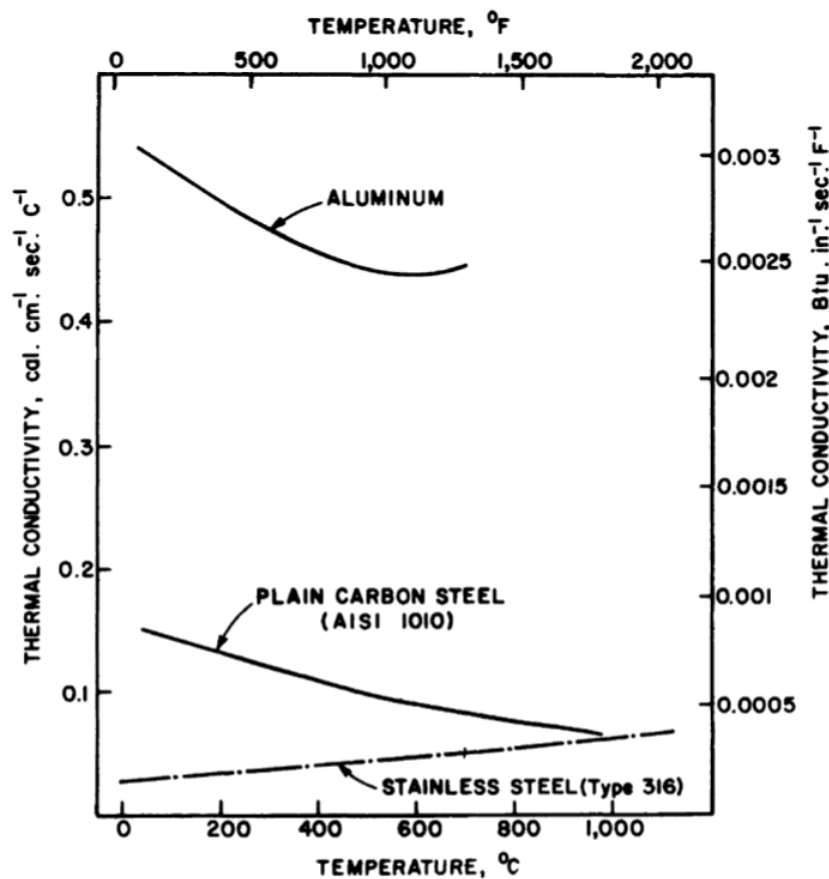


Figure 3 Thermal conductivity of steel and aluminium (Masubuchi 2013)

2.3.1 Gas Metal Arc Welding

Gas metal arc welding (GMAW), also referred to as metal inert gas (MIG) welding, is a method where an arch between an electrode and the workpiece metal is creating the heat for the weld. Continuous feeding and melting of the electrode contribute to filler metal addition (Figure 4). Bonding is achieved by mixing of the melted workpiece metal(s) and the melted electrode. The weld is protected by a shielding gas, often made of argon or helium.

Traditional GMAW have a relatively high heat input to the weld. To reduce the heat input a modified GMAW method called double-electrode gas metal arc welding (DE-GMAW) can be used. This technique uses a bypass torch which reduces the current needed to transfer droplets from the electrode to the workpiece. This method has been used to produce a relatively good lap-joint between aluminium and steel. In this case a maximum shear tensile strength of 88.5% of the aluminium base metal strength has been achieved (Shi et al. 2014). However, the average shear strength was significantly lower. The main advantage of the GMAW process is that its flexible and can quickly be used for many different types of welds. One disadvantage of GMAW is that it's not as energy efficient as the solid-state welding techniques, leading to degraded joint properties.

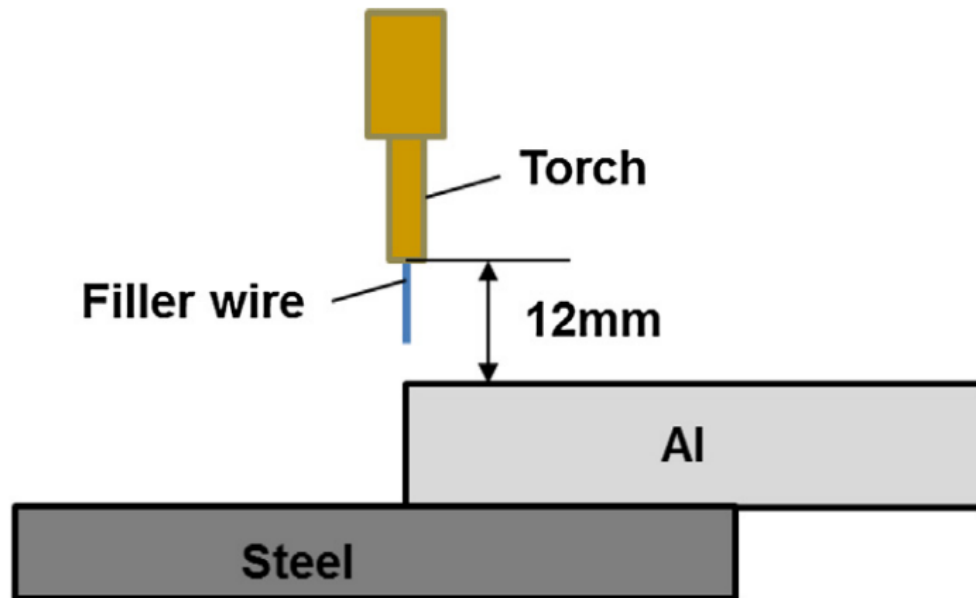


Figure 4 Simple illustration of how the GMAW and CMT uses a torch and filler wire in the weld (Yang et al. 2013)

2.3.2 Cold Metal Transfer welding

Cold metal transfer (CMT) welding, is a method developed by Fronius in Austria in 2004. The process has a low heat input and minimal spatter and is suitable for welding thin sheets. CMT is developed from GMAW and has some similarities. It forms an arc between the filler metal and the workpiece just like the GMAW method. However, the CMT process controls the material deposition by retraction of the wire. When the wire meets the weld pool the wire retracts and thereby initiating the droplet deposition. As the metal is transferred from the wire to the weld pool the current in the process is dropped to almost nothing. Then the current is brought back up the wire is put closer to the weld pool and a new droplet is transferred. This cycle is repeated multiple times every second (Furukawa 2006).

Cao et al. (2013) has compared an AA6061T6-galvanized steel weld and an AA6061T6-AA6061T6 weld, both produced using the CMT process. They got comparable results between the Al-Al weld and the Al-Fe weld. Both welds were weaker than the base aluminium, but the fracture occurred in the HAZ and not in the weld. This indicates that the Al-Fe interface is not the weakest point, and that the heat induced contribution to HAZ softening was the main problem. Minimizing the heat input will result in a smaller HAZ and a stronger joint (Cao et al. 2013).

2.3.3 Friction Stir Welding

Friction stir welding is a solid-state welding technique that is often used to join materials that are normally difficult to weld. The process is done by placing a rotating tool between two pinned plates (base materials). The tool then moves along the common edge of the plates using heat from the friction and plastic deformation of the materials to create bonding (Figure 5)

When joining aluminium and steel with FSW the pin is often put in with an offset so that most of the pin will machine the aluminium and just a bit of the steel. Resulting in less wear and less energy input (Watanabe, Takayama, and Yanagisawa 2006). Crack initiation and propagation in the brittle inter metallic compound (IMC) is still the driving force of fracture (Wang et al. 2018). However, Wang et al. still managed to produce an aluminium-steel FSW with a joint strength of up to 90% of base aluminium.

Welding speeds must be lower in FSW than in HYB welding to keep the temperature down. Still there are higher weld defects at the Al-Fe interface for FSW than in HYB welding. Wang et al. (2018) describes some welding defects in Al-Fe FSW welding, like voids and cracks along the Al-Fe interface (Wang et al. 2018). Fracture also occurs along the Al-Fe interface.

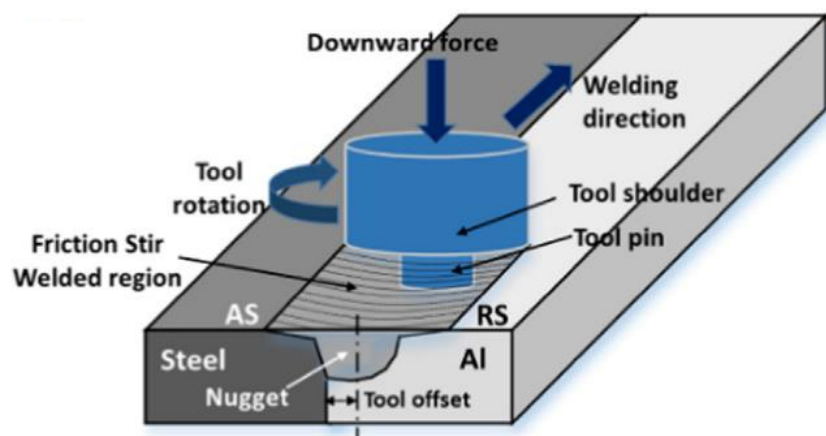


Figure 5 Illustration of FSW between Aluminium and steel (Wang et al. 2018)

2.4 Hybrid Metal Extrusion and Bonding (HYB)

Hybrid metal extrusion and bonding (HYB) is a bonding process that uses filler material and conform extrusion (Etherington 1974), to form bonding. Filler wire is extruded thru a pin and deposited on the base material. HYB is a method that uses some the best parts from the other welding processes. Using a filler wire like CMT and GMAW and still being a solid-state welding method like FSW. Making it possible to maintain a high welding speed. As previously mentioned, the process was at first intended to preform Al-Al butt welds. Which it has done with good results (Sandnes et al. 2019). But it has been developed further and is now able to create bonding between dissimilar materials. HYB can make strong Al-Fe joints with an extremely thin IMC, reducing the impact of the brittle compound (Grong, Sandnes, and Berto 2019a).

HYB is a solid-state welding process with multiple possible applications. Currently there is research being done checking these applications and where this process can be used. In this report the process of joining aluminium and steel is in focus. This chapter will give a simple walk through of the different generations of HYB Al-Fe welds.

The bonding in HYB is as mentioned intermetallic between the aluminium and steel. However, Al-FM and Al-BM is joined with metallic bonding. Occurring because of the shear deformation, oxide dispersion and pressure between the filament metal and the base aluminium.

2.4.1 First Generation Al-Fe HYB Welds

Joining of aluminium and steel produced using the HYB method is not an old method. However, there have already been some development from the first method to the current. In the first generation HYB Al-Fe welds the tool was conic, causing the need for pre machining of the steel. The aluminium was not pre machined and put a bit onto the path of the tool (Figure 6). Aluminium was placed on the advancing side of the weld while steel was put on the retreating side.

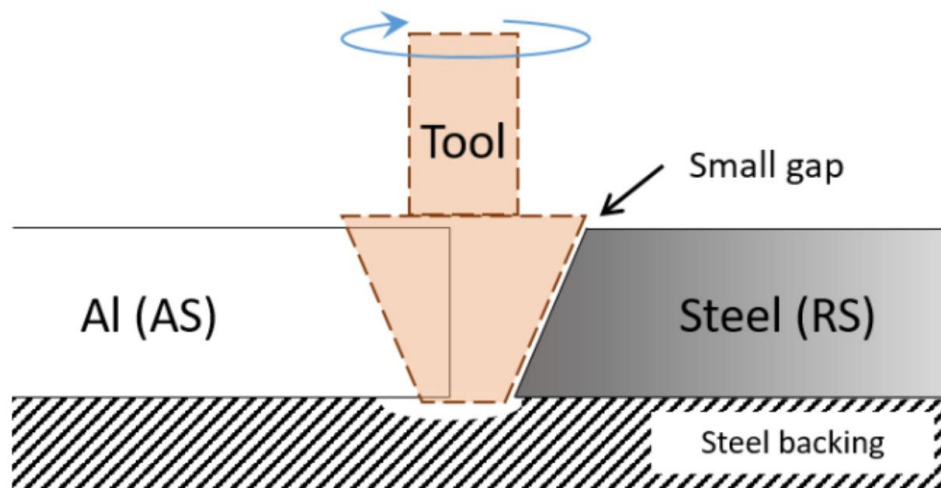


Figure 6 Visualization of the pin placement and geometry for the first generation Al-Fe HYB-welds (Berto et al. 2018)

The first generation HYB welds had relatively low strength compared with tensile strength of the base material, with an UTS in the weld that corresponds to about 45% of the base material aluminium UTS. However, the results were promising. It was found that the crack mainly propagated in the aluminium filament material and not in the IMC (Figure 7). Indicating a strong bonding in the Al-Fe interface and showing potential for the HYB produced Al-Fe weld. Berto et al. (2018) describes the experimental procedure and full results from the first generation Al-Fe HYB welds (Berto et al. 2018).

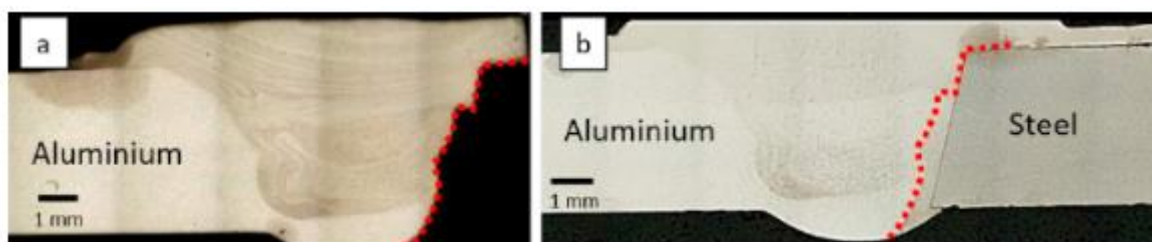


Figure 7 Images of the weld with a red dotted line indicating the fracture path shown on (a) a broken tensile specimen (b) an intact tensile specimen. Showing how most of the fracture occurs in the aluminium (Berto et al. 2018)

2.4.2 Second Generation Al-Fe HYB Welds

The HYB-welds from the second generation was made by a conic pin (Figure 8), this required some pre-machining of the steel side of the weld, for the pin to not intervene with the steel. Here the steel is put on the advancing side and aluminium on the retreating side of the weld.

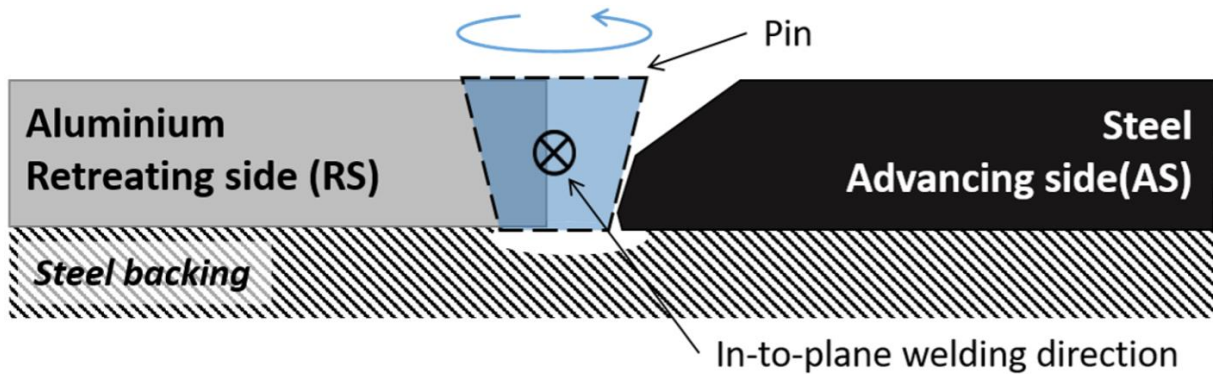


Figure 8 Visualization of the pin placement and design for the second generation of HYB-weld (Mathiasson 2019)

The aluminium and steel have changed sides compared with the first-generation Al-Fe HYB welding. One of the main problems this generation of HYB-welds had was lack of bonding in the Al-Fe interface close to the weld root. Fractures from the tensile tests of this weld normally occurred in the Al-Fe interface. Originating from the pre-existing cracks close to the weld root. The cracks propagated along the IMC between the aluminium and steel (Figure 9).

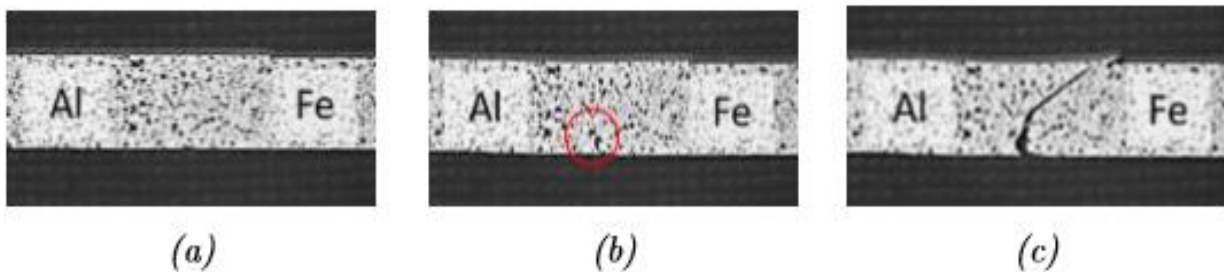


Figure 9 Crack propagation during tensile test; (a) start of loading, (b) visible crack initiation, (c) final fracture (Mathiasson 2019)

Average tensile strength on the second-generation welds are 228 MPa giving it a joint efficiency of approximately 75%. The joint efficiency on the tensile specimen with reinforcements (not flush-machined) reached 80%. Making the second-generation significantly better than the first, as previously mentioned had a joint efficiency of 45%.

2.4.3 Third Generation Al-Fe HYB Welds

There has been a development in the HYB process in the last year. Third generation HYB weld is made by using a circular pin (Figure 10). This removes the need for pre-machining of the steel that was necessary in the last generation. With this design the gap between the steel and the pin is the same in the full height of the weld. Welding defects like lack of bonding at the weld root, that the second-generation welds struggled with, have been reduced. This design has shown great results, increasing the yield strength of the joint and moving the fracture from the Al-Fe interface to the HAZ in aluminium (Sandnes, L. Personal communication 2019).

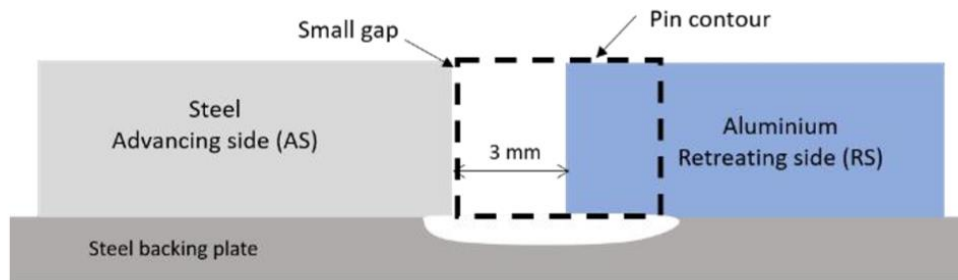


Figure 10 Visualization of pin placement in 3. generation HYB-welds (Grong, Sandnes, and Berto 2019a)

Test results from the third-generation Al-Fe HYB welds are yet to be published. However, the strain data from one of the specimens can be seen in Figure 11. The strain is concentrated in the HAZ and not in the Al-Fe interface. It also shows that the stain has an incline and is not vertical in the HAZ. A clear necking can be seen before fracture.

The final fracture also occurred with an incline in the HAZ. Flush-machined specimen reached an engineering UTS of 242.5 MPa giving this specimen a joint efficiency of 79%. Making an even better joint than the second-generation weld. And moving fracture from Al-Fe interface to the HAZ (Sandnes, L. Personal communication 2019).

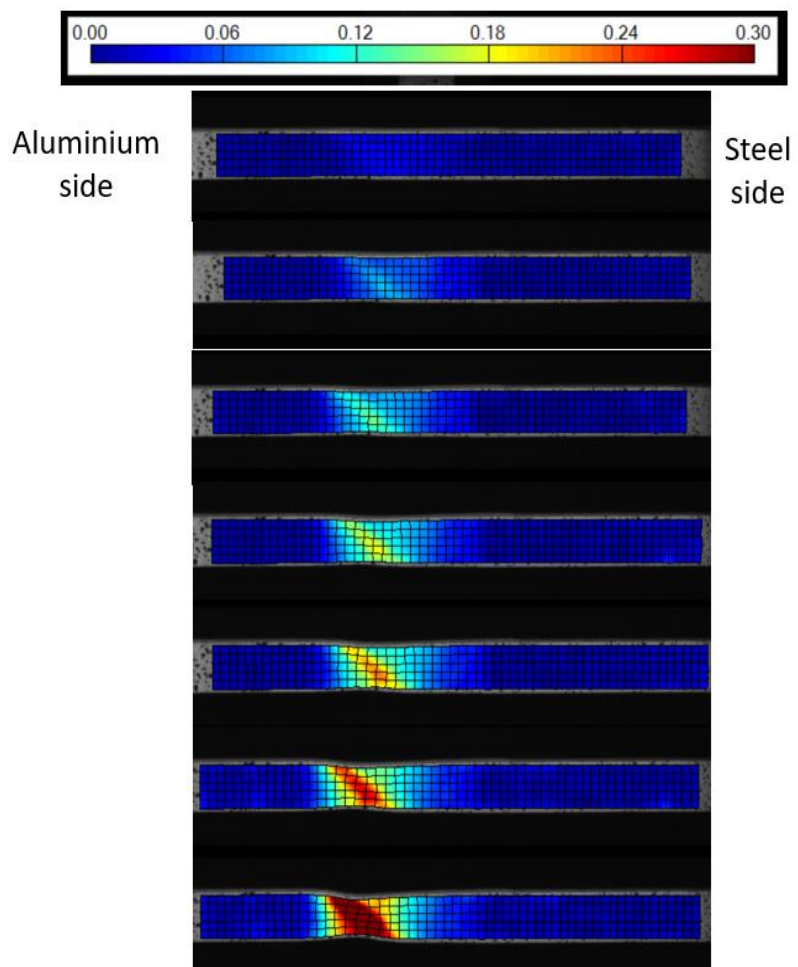


Figure 11 Strain development from tensile test. Results are visualised using DIC results, with strain going from 0 to 0.3 (Sandnes, L. Personal communication 2019)

2.5 Finite element method (FEM)

Finite element method or FEM is a method that uses numerical calculations to approximate engineering and mathematical problems. This is done by dividing the area of interest in a mesh. The mesh then contains nodes giving the model a finite number of points that are used to approximate the results. There is a variety of different versions of FEM. For example, extended finite element method that can be used to analyse cracks.

FEM has become a tremendous tool in engineering with many applications. Being able to calculate complex problems and get out stress, deformation and flow more accurately and a lot faster than by hand.

Many different types of elements can be used in FEM simulations (Figure 12). For the FE-models in this report linear solid hexahedral elements have been used to represent the tensile test specimen.

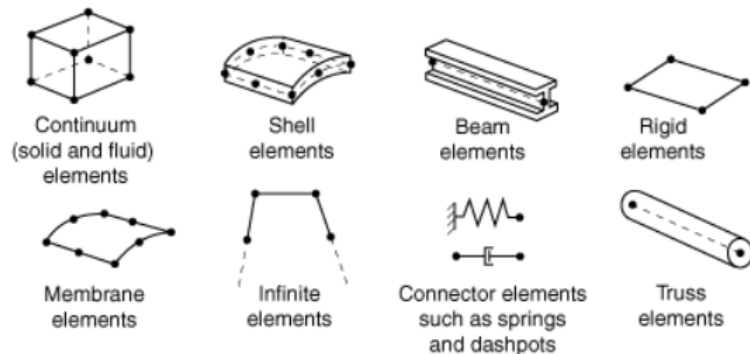


Figure 12 Commonly used element families (Abaqus-manual 2010)

2.6 In-Depth Review of the Second Generation FE-Model

Some of the previous work done to simulate HYB-welds has been a finite element (FE) model that Marie Mathiasson developed in her master thesis, in the spring of 2019 (Mathiasson 2019). This chapter is a review of the model in order to verify the results and evaluate parts that need improvement. The FE-model is built to simulate the strength in the joint made by second generation HYB-weld. And will therefore have some differences in results from the new model which is based on the third generation of HYB-welds.

2.6.1 Setup of the Model

The model was split in three parts, aluminium base material (Al BM), extrusion zone (EZ)/Heat affected zone (HAZ) and steel base material (Fe BM) (Figure 13). The EZ and HAZ is merged into one zone because of similar hardness and was given properties from a digital image correlation (DIC). The material data for Al BM and Fe BM are standard and taken from tables. One of the problems with merging the EZ and HAZ in the FE-model is that you neglect the difference in properties in the HAZ and EZ. It makes the weakest area of the weld larger than in reality, and the contest between a ductile fracture in the HAZ and crack propagation in the weld toe (EZ) will be hard to display.

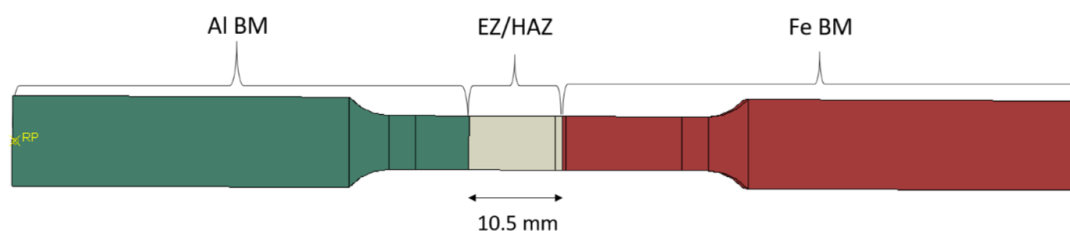


Figure 13 Illustration of the different sections in the FE model and materials assigned to them (Mathiasson 2019)

This model has chosen to focus on the crack and crack propagation in the aluminium close to the Fe-BM, since most of the tests broke in this area. This setup is sufficient for simulating the crack but has problems simulating necking and ductile fracture.

To simulate the crack propagation, the well-known method XFEM was used. XFEM or Extended finite element method is a method to simulate crack propagation that allows the crack to grow independent of the mesh (Belytschko and Black 1999). Maximum principal stress criterion was chosen in the model as a fracture criterion. The highest value of true ultimate tensile strength gathered from the DIC was used as maximum stress. The crack had to be placed with an offset from the Al-Fe interface in order to make the crack propagate in the Al, and not diverge into the steel side of the weld. From the backscattered electron (BSE) micrographs in Figure 14, taken from the fracture surface. There can be seen relatively large amounts of aluminium. Therefore, the offset of the crack from the Al-Fe interface is not seen as a large problem. Even though the crack is propagating closer to the steel side in the tests than in the simulation.

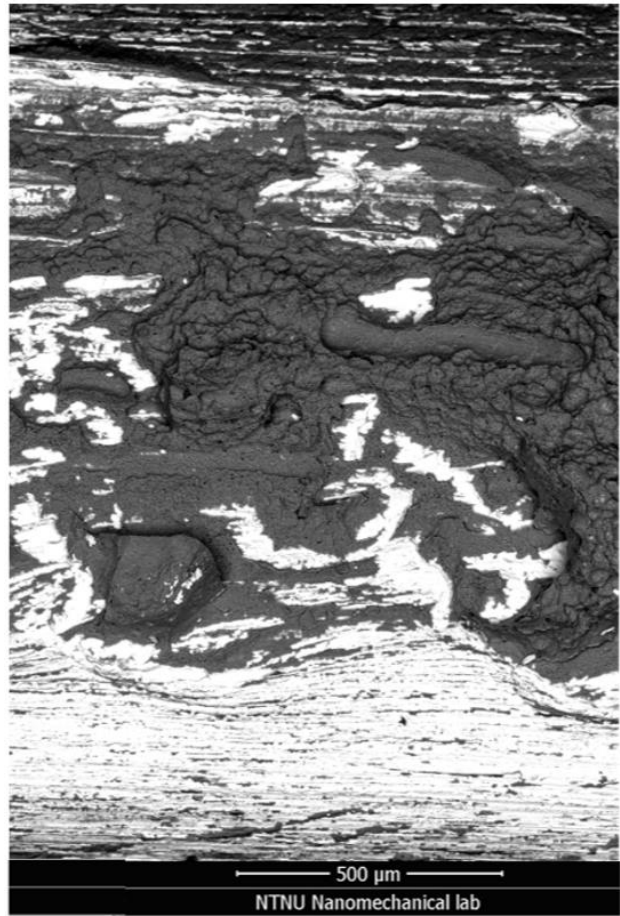


Figure 14 BSE micrographs at 100x magnification taken from the fracture-surface close to the weld root (Mathiasson 2019)

The loads and boundary conditions put on this model was fixed in one end and a forced displacement in the other. The boundary conditions were put on the same surfaces that are fixed during the tensile test.

The mesh used in the model is 8-node linear hexahedral elements with a size of 0.4mm in the EZ/HAZ and a global mesh size of 1mm for the rest of the model (Figure 15). The simulation was set up as a static general simulation. It was attempted to do a co-simulation using dynamic explicit to simulate the ductile damage in the HAZ and dynamic implicit to simulate the crack propagation. However, this resulted in large deformation in the interface and no valid results (Mathiasson 2019).

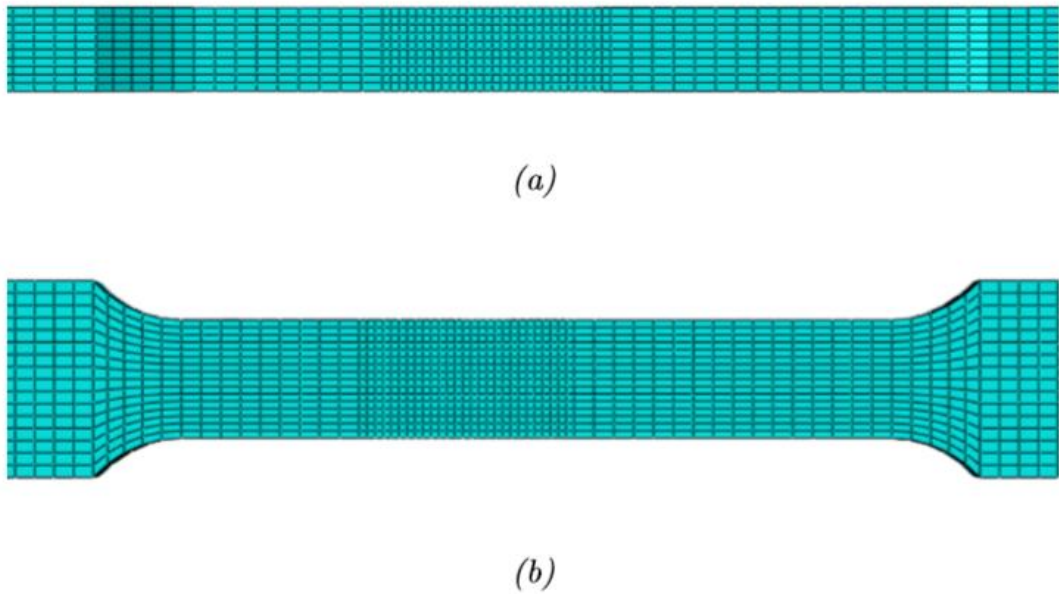


Figure 15 Mesh of the FE model; (a) in the thickness, (b) in the width of model (Mathiasson 2019)

2.6.2 Simulation Results

The main objective of this FE-model was to find out how different initial crack lengths influenced the fracture. Many different initial cracks were simulated, and the results are shown in Figure 16. Here we can see how the initial cracks gradually reduces the integrity of the weld, as expected. However, the simulation does not take into account that a fracture might occur in the HAZ when the cracks are small.

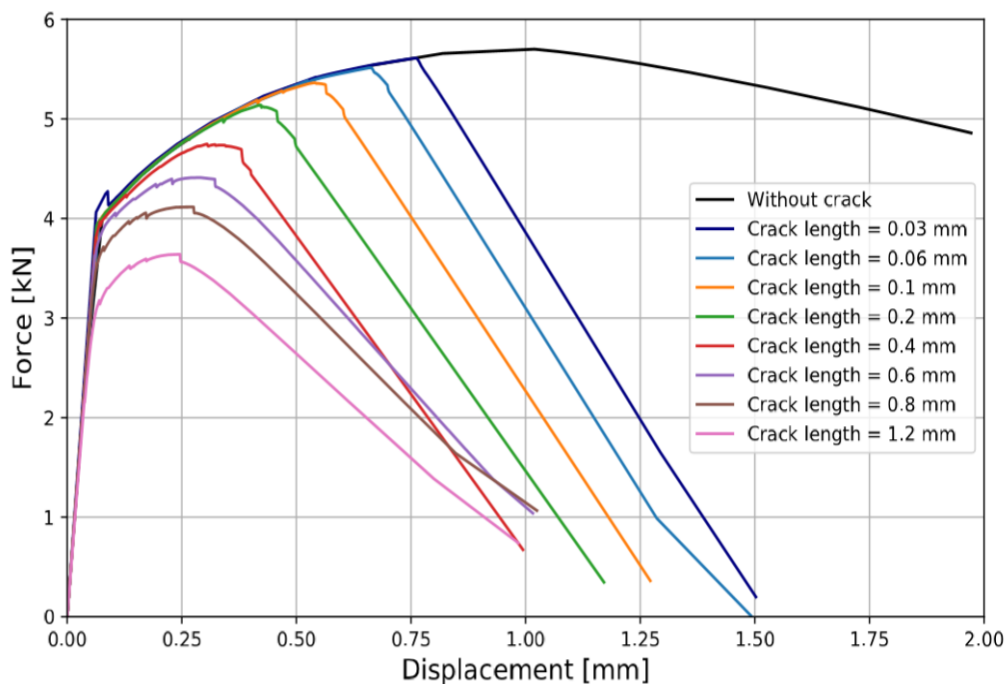


Figure 16 Plot showing the influence different initial cracks have on the fracture behaviour of the joint (Mathiasson 2019)

2.6.3 Needed Improvements

Even though this FE-model is relatively good and can produce results similar to the test results, there are a few points that need improvement. One thing that needs to be looked into is the E-modulus gathered from the DIC. The data from the virtual extensometer in the DIC is fluctuating and choosing to calculate the E-module from one point can give an incorrect E-module. Normal for aluminium is about 70GPa. However, in the FE-model an E-module of 43.87GPa was used in the HAZ.

The crack will create a stress concentration and with only one fracture criterion, make the fracture occur at the weld root no matter how small the initial crack is. When looking at the strain development in the simulation from Figure 17 a), with a large initial crack, strain development seems realistic. However, when the initial crack is small the strain is concentrated in the HAZ. Indicating that a ductile fracture might have occurred if it was included in the model. But in this simulation the crack still propagates in the Al-Fe interface as seen in Figure 17 b).

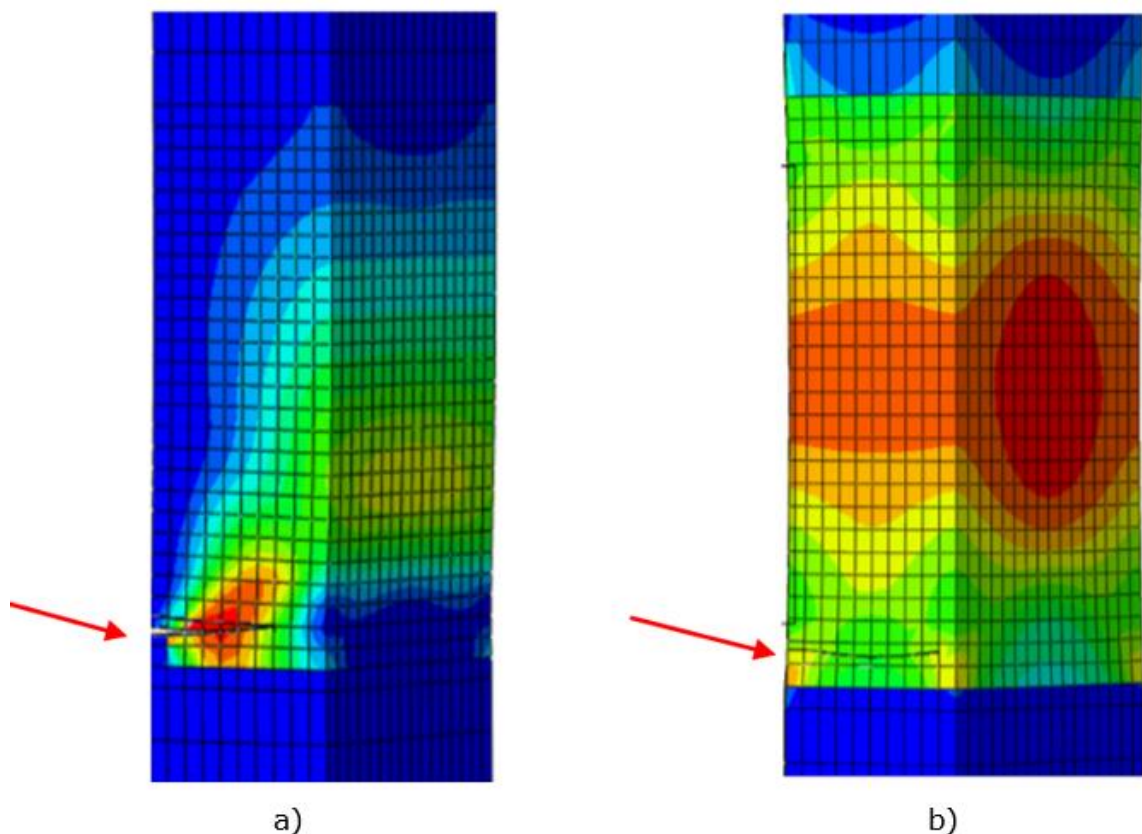


Figure 17 Strain in the simulation right before the final fracture for (a) a large initial crack of 0.8mm (b) a small initial crack of 0.03 mm (Mathiasson 2019)

Another simplification done on the model was the Al-Fe interface. In reality that interface is bent as seen in Figure 8. But in the FE-model the interface is represented as a straight vertical line. This will result in a difference in the stress and strain around the Al-Fe interface. The influence of this needs to be investigated further.

3 FE-Modelling of Third Generation Al-Fe HYB Weld

The objectives behind making a FE-model of the HYB-weld is to be able to compare and affirm the results from the tensile tests. And maybe get a better understanding of the fracture when we can see how the stress develops throughout the weld. The FE model will also be able to quickly analyse the influence of different defects and changes in the weld. This model will work as a base for further development in a master thesis in the spring of 2020.

3.1 Setup of the Model

3.1.1 Partitioning of Different Zones

After finishing the in-depth review of the existing model. The work on making a new model started. The first thing needed to be done was to figure out what zones to partition the weld into and find a placement for the different zones. From Figure 18 a preliminary partition of the different weld zones can be seen. To be able to better show the stress and strain in the weld the EZ and the HAZ in the aluminium was split in two zones. Unlike in the second generation weld that had merged EZ and HAZ. The HAZ at the steel side was neglected and given the properties of the steel base metal because of the low temperature in the weld and the strength difference between steel and aluminium.

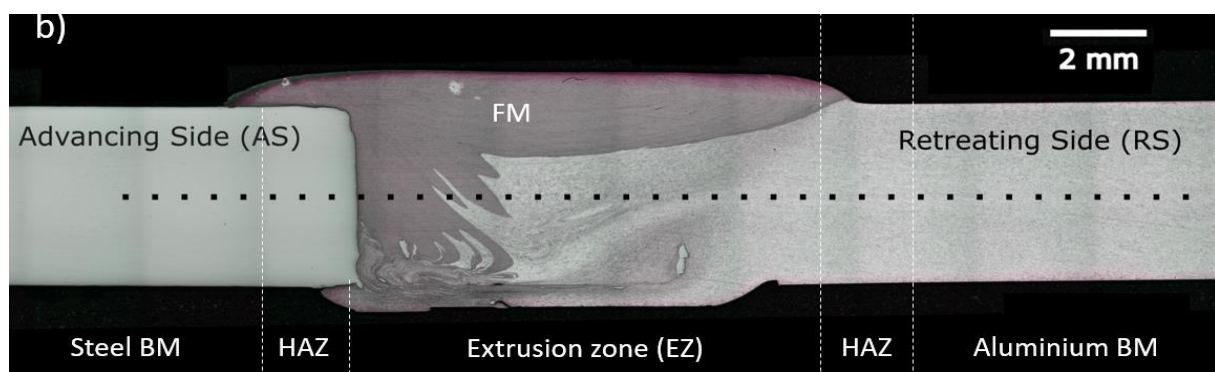


Figure 18 Preliminary partition of the different zones within the weld (Sandnes, L. Personal communication 2019)

Over to the placement of the different zones. The boundary between Fe-BM and EZ is a simple vertical line, because of the cylindrical shape of the pin. To find a placement of the HAZ, hardness data collected by Lise Sandnes was used. Hardness data was taken at three different heights in the weld, across all the weld zones. Average hardness values were put in a table shown in Figure 19. There is a dip in hardness indicating a weaker zone in the aluminium. This is assumed to be the HAZ. The dip in hardness has an incline. This can best be seen in the hardness plot from Figure 20. Where it's clear that the drop in hardness

is deeper in the aluminium side of the weld at 1mm over center than 1mm under center of the weld. Indicating that the HAZ is not vertical but inclined through the weld. From this data the start of the HAZ is chosen to be six millimeters from the Al-Fe interface at center of the weld with an incline of 45 degrees.

	-5	-4	-3	-2	-1	0	1	2	3	4	5	6	7	8	9
1	225,73	191,30	100,40	102,43	97,53	97,93	95,43	93,93	89,30	85,63	81,80	86,87	97,37	113,07	123,53
0	215,83	171,27	90,80	90,93	88,17	84,90	86,13	85,67	78,27	82,70	83,20	88,30	99,33	118,00	119,70
-1	213,67	164,63	83,80	88,37	87,80	87,03	87,03	79,37	75,30	88,60	93,73	99,27	107,90	120,87	125,40

Figure 19 Average hardness data taken at different points in the weld. 1, 0 and -1 on the left indicates hardness data taken 1mm over centre, in the centre and 1mm under centre of the weld thickness. (full table can be found in appendix A)

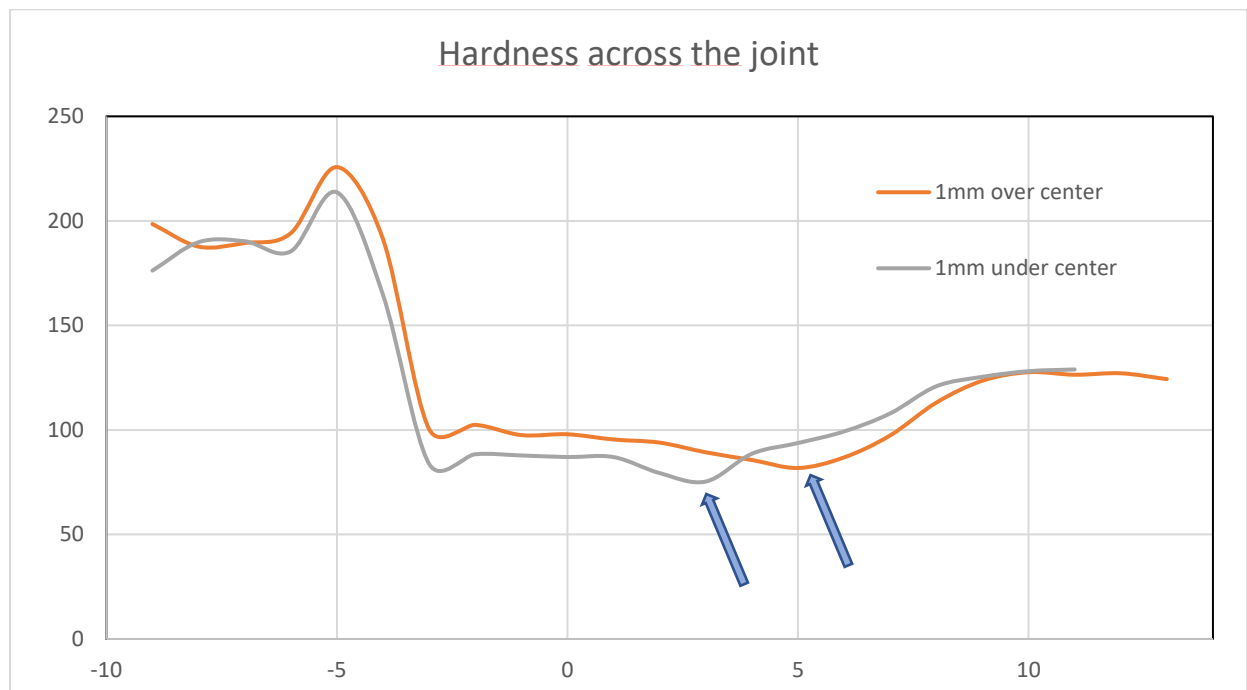


Figure 20 Hardness data plot for 1mm over and 1mm under centre of the weld. Arrows indicating the HAZ placement

To find the width of the HAZ a method based on Mazzolani (1994) and previously used by Myhr and Grong (2009) was used to calculate the reduced strength zone (Mazzolani 1994), (Myhr and Grong 2009). The relationship between hardness and yield strength from equation 1 was used to gather preliminary strength values. Then used in equation 2 to calculate the reduced strength zone.

$$(1) \quad \sigma_{ys} = 3.0HV - 48.1$$

Equation 1 Relationship between hardness and strength

$$(2) \quad \Delta y_{red}^{eq} = \frac{\int_{y_m}^{\infty} (\sigma_b - \sigma) dy}{(\sigma_b - \sigma_{min})}$$

Equation 2 Reduced strength zone (Mazzolani 1994)

The calculations were done for all three heights in the weld. And resulted in the data seen in Table 1. The full calculations can be found in appendix A. The width of the HAZ was chosen to be four millimetres across the weld to simplify the model.

	Δy_{red}^{eq}
1	3,90mm
0	4,49mm
-1	4,29mm

Table 1 Reduced strength zone at three different heights in the weld.

This resulted in a model with the different zones as seen from Figure 21. The basics of this FE model and simulation are built the same way as in the previous model. With constraints working on the surfaces connected to the machine in the tensile test. And a forced displacement put on one side.

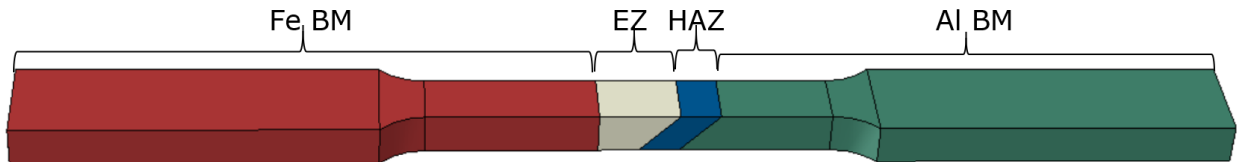


Figure 21 Illustration of the different sections in the FE model and materials assigned to them.

Since the basics of the FE model is the same as for the previous one, a quick test was done to affirm the results from the previous model. And to check that the setup for the new model is working. Old material data (from the previous FE model) were assigned to the new model and a simulation was done. The results from this simulation should be comparable with that of the previous model without a pre-existing crack. From Figure 22 and Figure 23 the difference in the results can be seen. 32N in difference is just over 1MPa. Indicating that the setup of the model is working and affirming the results from the previous model by reproducing them.

Old model

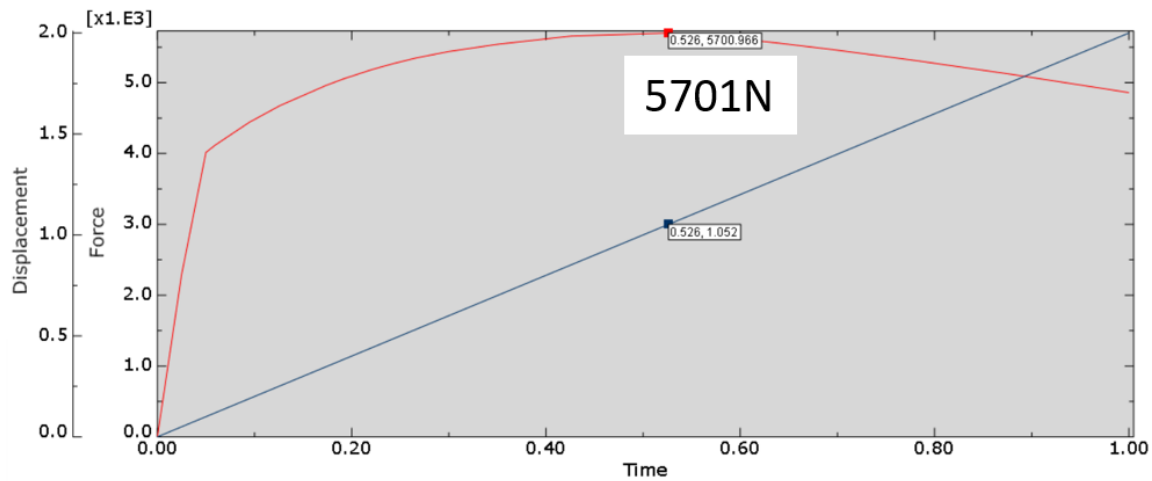


Figure 22 Displacement and maximum force on the old FE model without a crack

New model

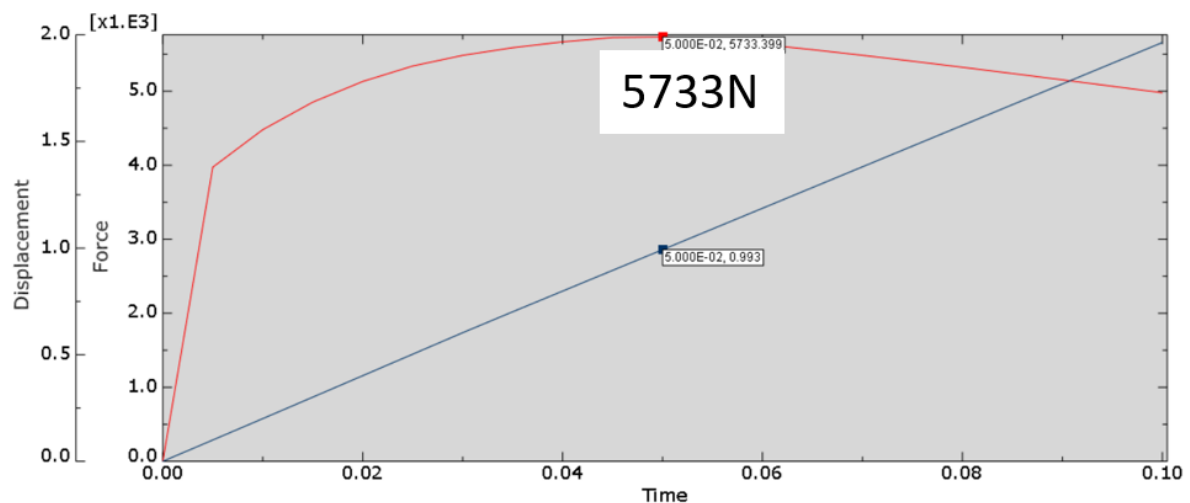


Figure 23 Displacement and maximum force on the new model without a crack

3.1.2 Materials Data

Choosing the sections needed in the model and finding the correct placement of them are one thing. But to make a FE-model for the 3. Generation new materials data was needed. Because of the new welding method and because of the splitting of HAZ and EZ. Al-BM and Fe-BM was given data from the known base materials. In order to find the data for the HAZ and the EZ virtual extensometers was placed on the DIC. One extensometer covering the EZ and one over the HAZ (Figure 24).

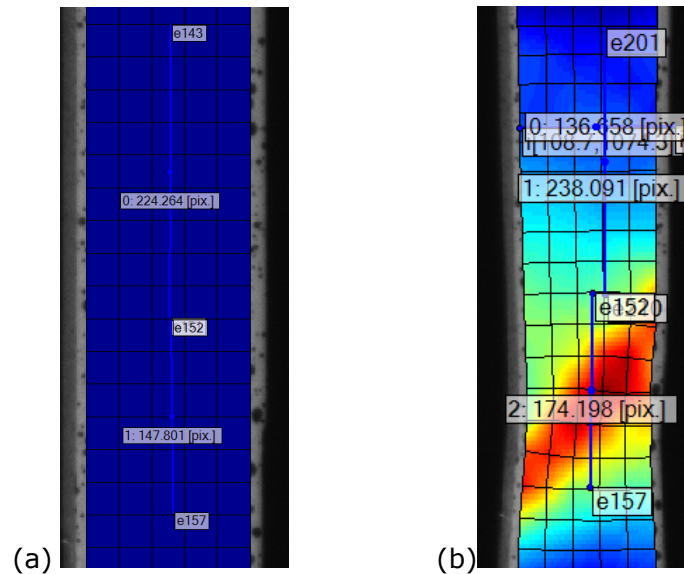


Figure 24 Screenshots showing the placement of the virtual extensometer over the EZ (top) and HAZ (bottom) at (a) before loading without strain (b) after loading with strain

The result from the virtual extensometers were then exported to excel and converted to stress and strain. The true stress plastic strain data for the HAZ was possible to obtain directly from the DIC. Because this is the weakest point and we get the full stress strain curve from start of loading up until fracture. However, from the engineering stress strain curve in Figure 25 we can clearly see a break in the curve for the EZ. This occurs because of strain concentration in the HAZ after it reaches its UTS, making the data for EZ only valid up until the HAZ-UTS.

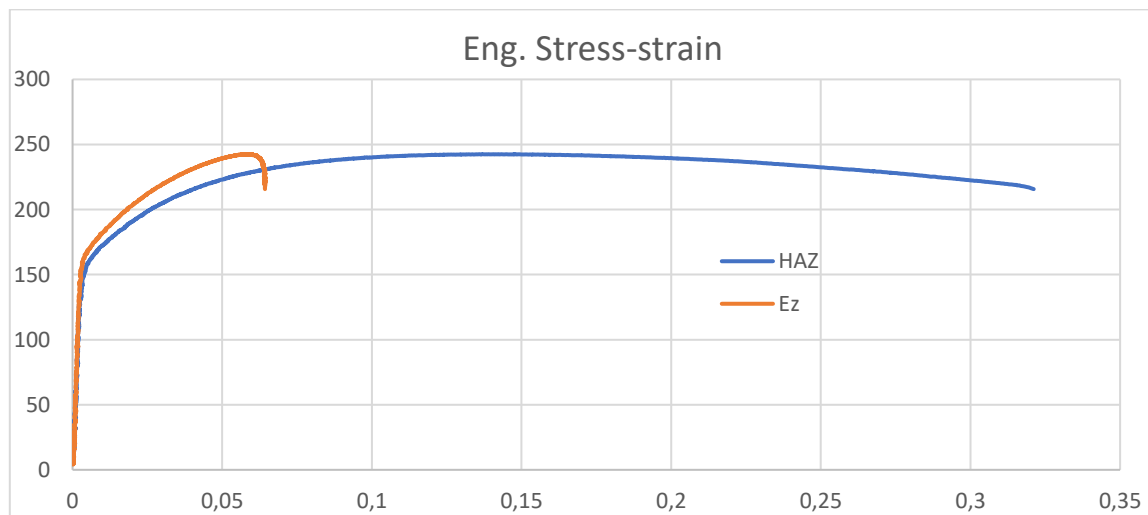


Figure 25 Engineering stress strain curve for HAZ and EZ obtained from DIC results

Another method had to be used to obtain the needed true stress plastic strain data for the EZ. Since the EZ is a mixture between FM and HAZ material the concept "rule of mixtures" was used. Where weighted parts of the materials are combined to find the strength of the mixture. Material data for the FM where obtained from a test SINTEF had done on this material previously (Figure 26). And combined with the HAZ material data from the DIC.

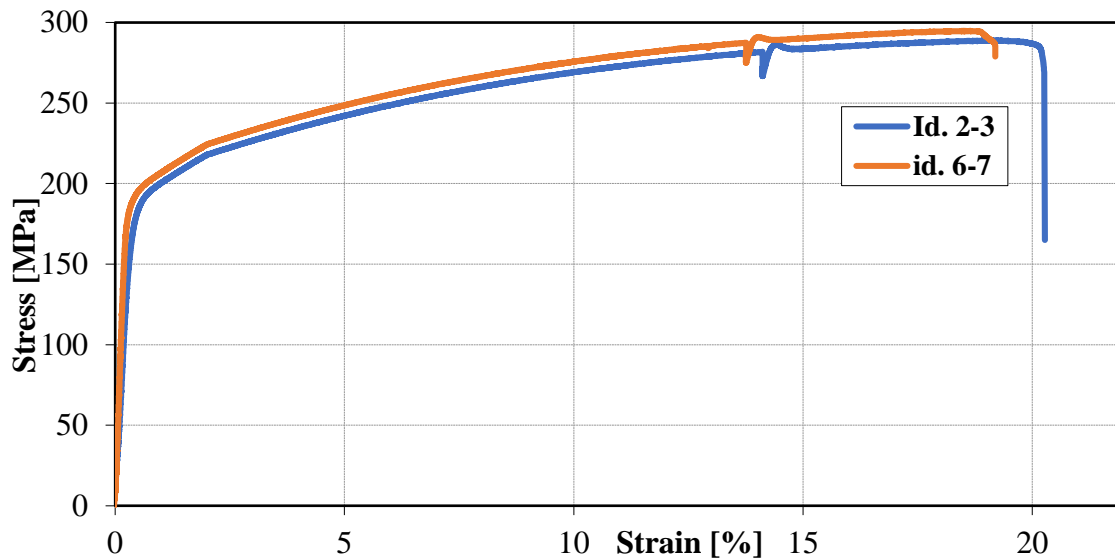


Figure 26 Stress-strain data for FM copied from SINTEF test done to the same FM on a previous occasion (SINTEF 2018)

Assuming that the whole void is filled with FM and that all the FM is in the EZ the weighted percentage of FM and HAZ material could be obtained. The area of the EZ in the model is 24mm^2 (seen from the side). The gap between the aluminium plate and the steel plate before welding was 3mm and the thickness of the weld is 4mm. Making the void area 12mm^2 and making the mixture 50/50 between filament and heat affected material. The materials data were then combined to gain the true stress plastic strain data needed for Abaqus (Figure 27).

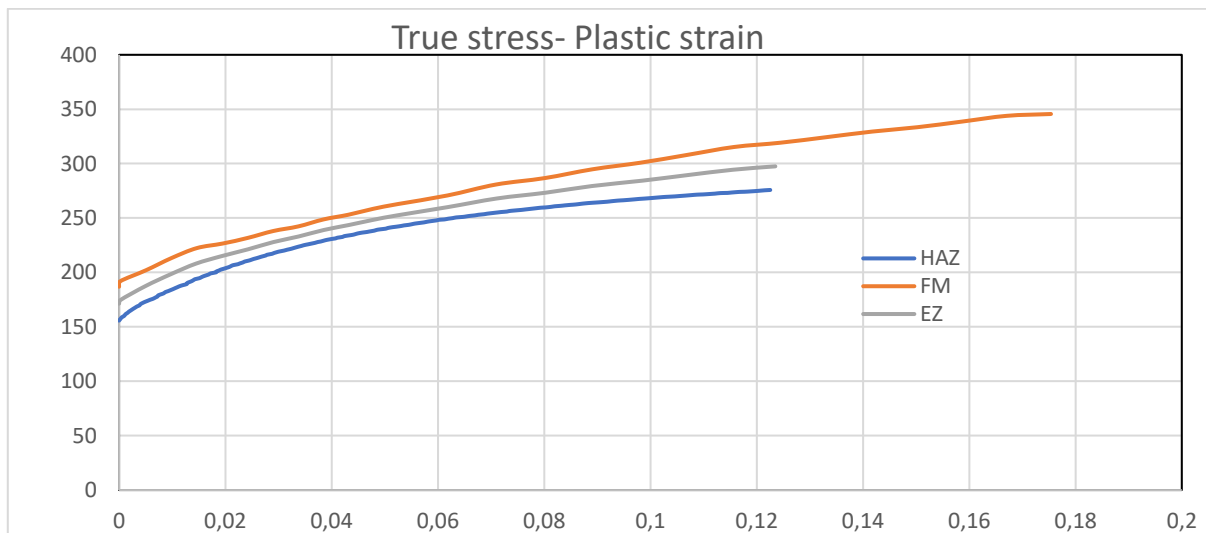


Figure 27 True stress plastic strain data for HAZ, EZ and FM

With all the materials data included in the model the setup of the new simulations could start. The fracture criterion, ductile damage with element deletion was chosen. Because the fracture in the tensile tests were placed in the ductile HAZ of the aluminium. Fracture strain in the HAZ was put at maximum strain from the DIC (0.27). Stress triaxiality was assumed to be 0.4 and the strain rate was put at a low value, because the rate has minimum influence in the tensile test. Because of the ductile damage criterion and element deletion the simulation was a dynamic explicit analysis.

The mesh used in the simulation was 8-node linear hexahedral elements with a maximum size of 0.5mm in the HAZ and EZ. Some elements were smaller in the EZ due to the inclined sections (Figure 28). For the Al-BM and Fe-BM a global mesh size of 1.5mm was chosen. The model was meshed using structural mesh controls. Resulting in a mesh consisting of 12120 linear hexahedral elements.

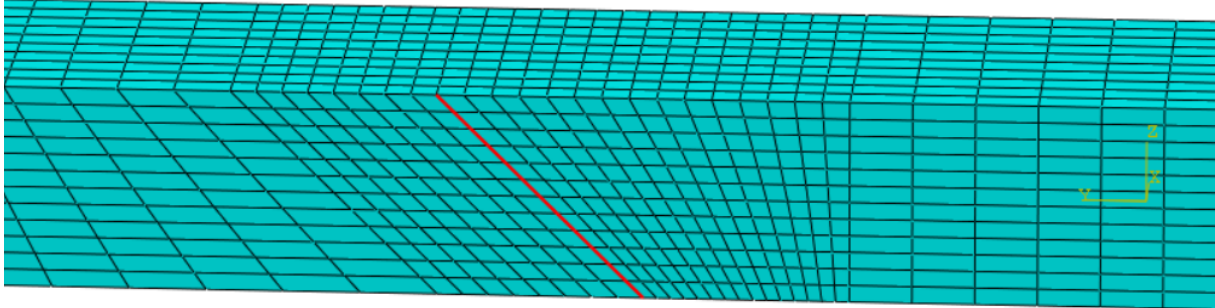


Figure 28 Mesh of the HAZ and EZ. With a red line indicating the interface between the sections

The forced displacement on the movable part of the specimen was put at 3mm. It was found that this was enough for fracture to occur. The displacement where applied to the model linearly over a timeframe of 0.1sec. All boundary conditions and loads where put on the model through a reference point at each end (Figure 29), making it easy to control and to extract data from the simulation.

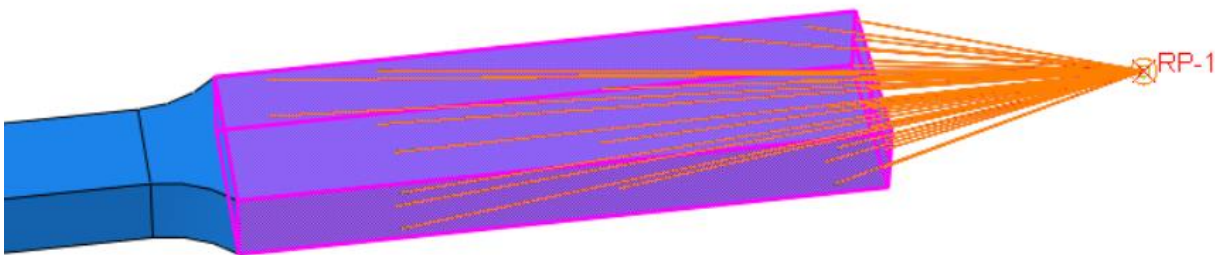


Figure 29 Reference point connected to surfaces on that are pinned in the tensile test used to apply boundary conditions and forced displacement

3.1.3 Simulation Results

Over to the results from the simulation. The reaction forces from the reference points show the reaction forces given the applied displacement. These forces can be compared with the force data from the tensile test results. Figure 30 show force and displacement throughout the simulation. A maximum force of 6045N equals an engineering UTS of about 252 MPa. Just under 10 MPa higher than the results from the tensile tests results presented in chapter 2.4.3 (242.5 MPa). This is not seen as a too large difference. However, it should be smaller. One of the reasons why UTS is higher in the simulation compared with the tensile test might be because of a stronger HAZ in the model. Or it can have something to do with the mesh, that will have to be looked into further.

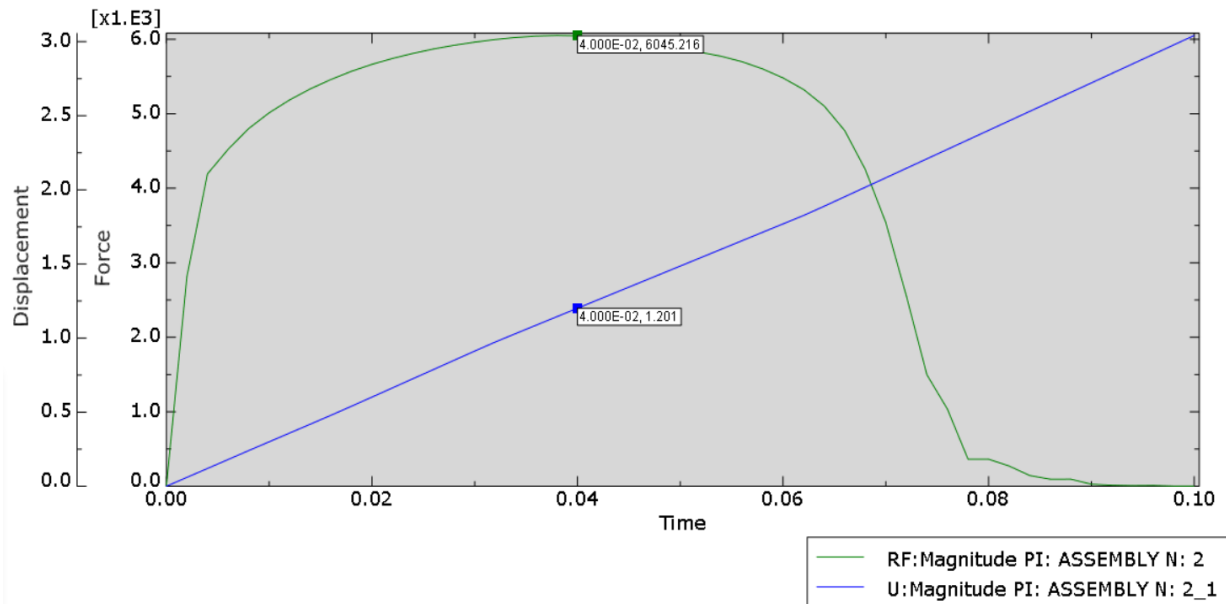


Figure 30 Reaction forces and displacement taken from the reference point where the forced displacement is applied

The strain development and distribution are important to analyse in order to understand where the weakest point in the weld is located. The strain is relatively evenly distributed in the HAZ and EZ at the beginning (Figure 31). Before more and more strain is concentrated in the HAZ. As was expected from the strain development in the tensile test DIC results. However, a clear boundary in the strain between HAZ and EZ can be seen in the simulation. This seems unnatural and probably occurs because of the rapid change of the materials properties between the zones. Effect of this clear boundary should be further investigated. To see if it has an influence on the simulation compared with the tensile tests or not.

There are no large plastic strains in any of the base materials. The steel base material, as you would expect shows close to no plastic strain at all. Aluminium base material did however show some plastic strain towards the end of the simulation, but not a significant amount (Figure 31).

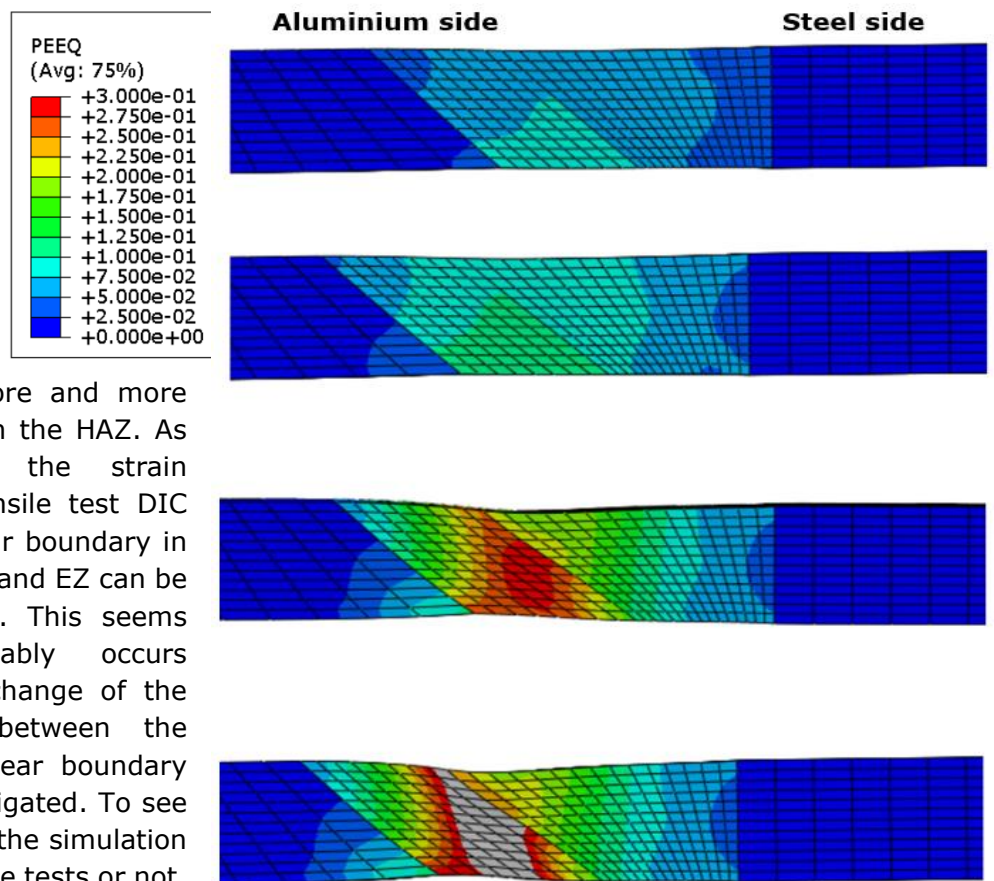


Figure 31 Equivalent plastic strain (PEEQ) development in the weld. From start of loading until right before fracture begins with a colour scale going from 0 to 0.3

The final fracture started at the top of the weld in the boundary between HAZ and EZ as seen from Figure 32. The figure also indicates that there are some shear forces in the weld. As the aluminium side of the fracture is "pushed" upwards. This might occur because of how the different zones are represented in the simulation.

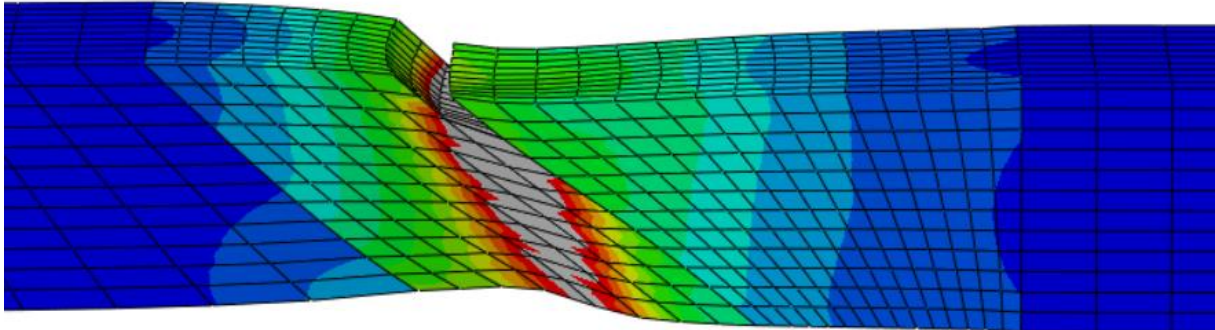


Figure 32 Start of the fracture with a PEEQ scale from 0 to 0.5

The final fracture occurred with an angle of about 30 degrees of the vertical axis (Figure 33). The mesh is rather large for element deletion, giving a crude fracture surface. The fracture went into the HAZ in the simulation, after having started in the interface between HAZ and EZ. It was expected that the fracture would go in the HAZ and not in the interface. This might have a relation to the strain concentration in the top of the specimen at the interface.

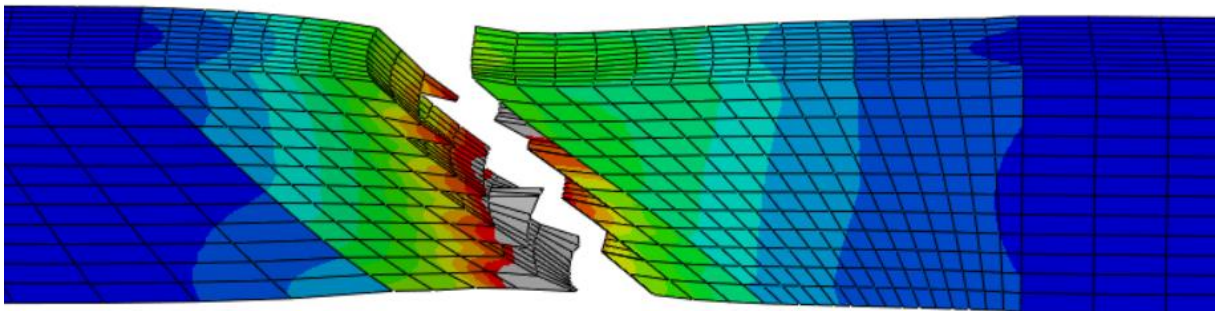


Figure 33 Final fracture of the test specimen from simulation with a PEEQ scale from 0 to 0.5

However, the fracture from the simulations (Figure 33) are very similar to the fracture of the tensile tests (Figure 34). This together with the similar strength indicates that the fracture behaviour is similar in the simulation and in the tensile tests. Making the FE-model a good starting point for further work.

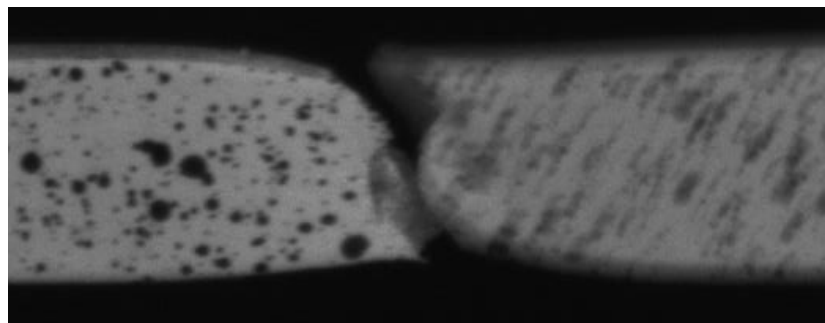


Figure 34 Final fracture of the test specimen from tensile testing (Sandnes, L. Personal communication 2019)

4 Conclusion

4.1 Concluding Remarks

It can be concluded from the literature review of different techniques of welding aluminium to steel, that the Hybrid Extrusion and Bonding (HYB) method are comparable, and on some aspects, even better than the existing methods. Having a great advantage in being a solid-state welding technique which gives a higher joint efficiency. The HYB method also has a high welding speed.

The in-depth review of the FE-model made by Marie Mathiasson showed some points that need improvement. For example, it needs further analysis of how the fracture behaviour changes with small initial crack with the possibility of fracture in the HAZ. However, there were a lot to learn from that model. And the results with larger initial cracks seems realistic, giving a good reproduction of the tensile test results with weld defects.

FE-model for the third generation AL-FE HYB welds show great promise. Strength and strain development are somewhat realistic. However, the clear line between strain in HAZ and EZ should be investigated further. As well as the strain concentration in the point where the fracture starts in the HAZ-EZ interface. Other than that, the simulation shows good results indicating that the model can be used in further development.

4.2 Further work

Further work is as mentioned to improve the model for third generation Al-Fe HYB-weld. By analysing the influence of the clear boundary between the HAZ and EZ, as well as the strain concentration where the crack begins.

One of the first things on the agenda is to become familiar with and use Weldsim, a tool to simulate welding, to gain additional knowledge about the weld. Gathering information like heat flow and residual stresses in the weld. In order to use this in the Abaqus model.

When all the new data and a crack propagation fracture criterion is implemented in the model. Initial cracks and weld defects should be included to evaluate critical crack lengths. Simulation of fatigue fracture behaviour should also be investigated. Residual stresses from the weld will be important in the fatigue behaviour of the weld and should be included in the fatigue simulations.

5 Citations

Abaqus-manual. 2010.

<http://130.149.89.49:2080/v6.10ef/books/usb/default.htm?startat=pt06ch24s01abo23.html>

Belytschko, T., and T. Black. 1999. 'Elastic crack growth in finite elements with minimal remeshing', *International Journal for Numerical Methods in Engineering*, 45: 601-20.

Berto, Filippo, Lise Sandnes, Filippo Abbatalini, Øystein Grong, and Paolo Ferro. 2018. 'Using the Hybrid Metal Extrusion & Bonding (HYB) Process for Dissimilar Joining of AA6082-T6 and S355', 13: 249-54.

Blindheim, Jørgen, Torgeir Welo, and Martin Steinert. 2019. 'First demonstration of a new additive manufacturing process based on metal extrusion and solid-state bonding', *The International Journal of Advanced Manufacturing Technology*: 1-8.

Cao, R., Gang Yu, J. H. Chen, and Pei-Chung Wang. 2013. 'Cold metal transfer joining aluminum alloys-to-galvanized mild steel', *Journal of Materials Processing Technology*, 213: 1753-63.

Drivealuminium, 2017. 2017. 'ALUMINUM CONTENT IN NORTH AMERICAN LIGHT VEHICLES 2016 TO 2028'.

Etherington, C. 1974. 'CONFORM—a new concept for the continuous extrusion forming of metals'.

Furukawa, K. 2006. 'New CMT arc welding process—welding of steel to aluminium dissimilar metals and welding of super-thin aluminium sheets', *Welding international*, 20: 440-45.

Grong, Øystein, Lise Sandnes, and Filippo Berto. 2019a. 'Progress in Solid State Joining of Metals and Alloys', *Procedia Structural Integrity*, 17: 788-98.

———. 2019b. 'A status report on the hybrid metal extrusion & bonding (HYB) process and its applications', *Material Design & Processing Communications*, 1: e41.

Gullino, Alessio, Paolo Matteis, and Fabio D'Aiuto. 2019. 'Review of Aluminum-To-Steel Welding Technologies for Car-Body Applications', *Metals*, 9: 315.

Lumley, R. N. 2011. '1 - Introduction to aluminium metallurgy.' in Roger Lumley (ed.), *Fundamentals of Aluminium Metallurgy* (Woodhead Publishing).

Masubuchi, Koichi. 2013. *Analysis of welded structures: residual stresses, distortion, and their consequences* (Elsevier).

Mathiasson, Marie. 2019. 'An In-Depth Analysis of the Bond Strength of a Dissimilar Al-Fe HYB (Hybrid Metal Extrusion & Bonding) Joint', Master thesis, NTNU.

Mazzolani, Federico. 1994. *Aluminium alloy structures* (CRC Press).

Myhr, OR, and Ø Grong. 2009. 'Novel modelling approach to optimisation of welding conditions and heat treatment schedules for age hardening Al alloys', *Science and technology of welding and joining*, 14: 321-32.

Praveen, P., and P. K. D. V. Yarlagadda. 2005. 'Meeting challenges in welding of aluminum alloys through pulse gas metal arc welding', *Journal of Materials Processing Technology*, 164-165: 1106-12.

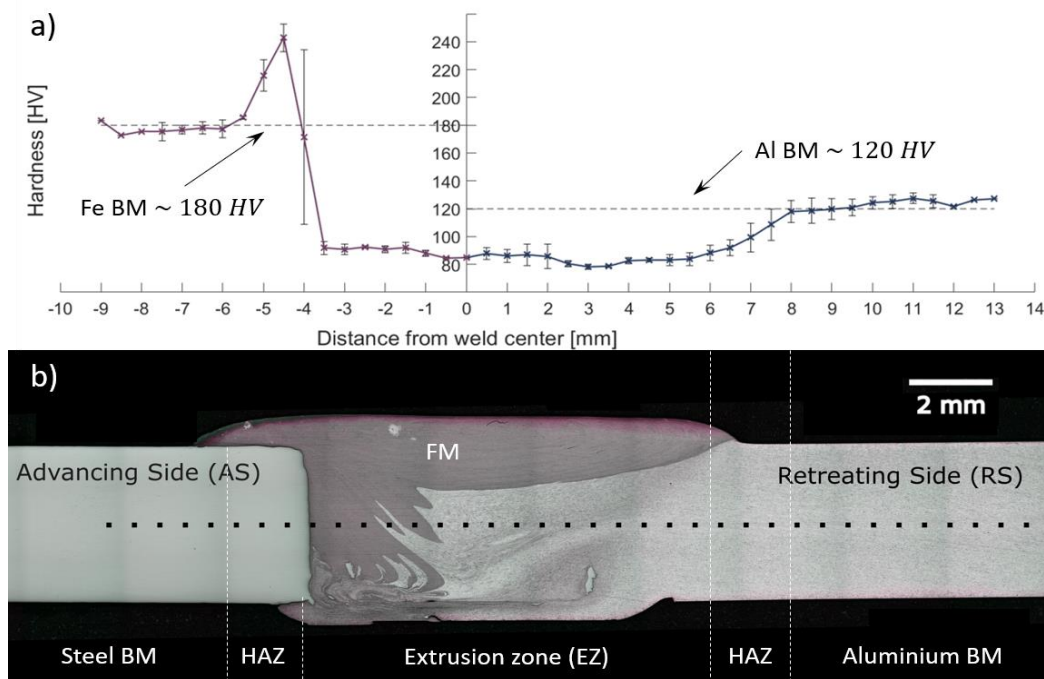
Sandnes, Lise, Luca Romere, Øystein Grong, Filippo Berto, and Torgeir Welo. 2019. 'Assessment of the Mechanical Integrity of a 2 mm AA6060-T6 Butt Weld Produced Using the Hybrid Metal

- Extrusion & Bonding (HYB) Process—Part II: Tensile Test Results', *Procedia Structural Integrity*, 17: 632-42.
- Shi, Y, G Zhang, Y Huang, L Lu, J Huang, and Y Shao. 2014. 'Pulsed double-electrode GMAW-brazing for joining of aluminum to steel', *Weld. J*, 93: 216-24.
- SINTEF. 2018. "Hardness measurement and tensile testing of all-weld HYB specimens." In.
- Soo, Vi Kie, Jef Peeters, Dimos Paraskevas, Paul Compston, Matthew Doolan, and Joost R. Duflou. 2018. 'Sustainable aluminium recycling of end-of-life products: A joining techniques perspective', *Journal of Cleaner Production*, 178: 119-32.
- Tanaka, Tsutomu, Taiki Morishige, and Tomotake Hirata. 2009. 'Comprehensive analysis of joint strength for dissimilar friction stir welds of mild steel to aluminum alloys', *Scripta Materialia*, 61: 756-59.
- The Lincon Electric Company, 1994. 1994. 'The Procedure Handbook of Arc Welding'.
- Total materia, 2003. 2003. 'Aluminum-Magnesium-Silicon (6000) Alloys', Accessed 04.12.2019. <http://www.totalmateria.com/Article74.htm>.
- Wang, Tianhao, Mageshwari Komarasamy, Kaimiao Liu, and Rajiv S Mishra. 2018. 'Friction stir butt welding of strain-hardened aluminum alloy with high strength steel', *Materials Science and Engineering: A*, 737: 85-89.
- Watanabe, Takehiko, Hirofumi Takayama, and Atsushi Yanagisawa. 2006. 'Joining of aluminum alloy to steel by friction stir welding', *Journal of Materials Processing Technology*, 178: 342-49.
- Worldsteel. 2019. "Worldsteel in figures 2019." In.
- Yang, Shanglu, Jing Zhang, Jin Lian, and Yongpin Lei. 2013. 'Welding of aluminum alloy to zinc coated steel by cold metal transfer', *Materials & Design*, 49: 602-12.

6 Appendix

6.1 Appendix A

Calculations on the HAZ, using hardness data for the weld to find the placement and width of the HAZ in the FE-model



Explanation of where the Centrepoin in hardness measurements is in relation to the different sections on the weld. (Sandnes, L. Personal communication 2019)

Hardness data from different weld specimens of third generation Al-Fe HYB welds, that where collected by Lise Sandnes, where then used to make the table below. Average values where used in the table to get the best possible overview. The HAZ is located a few millimetres away from the Al-Fe interface (the red zone). An incline in the HAZ can also be seen from the table below. In the centre of the weld a starting place for the HAZ was chosen at 6mm from the Al-Fe interface with an angle of 45degrees.

	-9	-8	-7	-6	-5	-4	-3	-2	-1	0	1	2	3	4	5	6	7	8	9	10	11	12	13
1	198,50	187,70	189,40	194,10	225,73	191,30	100,40	102,43	97,53	97,93	95,43	93,93	89,30	85,63	81,80	86,87	97,37	113,07	123,53	127,63	126,40	127,10	124,30
0	183,30	175,60	176,63	177,33	215,83	171,27	90,80	90,93	88,17	84,90	86,13	85,67	78,27	82,70	83,20	88,30	99,33	118,00	119,70	124,40	127,53	121,70	127,20
-1	176,20	189,80	190,27	185,43	213,67	164,63	83,80	88,37	87,80	87,03	87,03	79,37	75,30	88,60	93,73	99,27	107,90	120,87	125,40	128,10	128,93		

Full table of average hardness data at different points in the weld. With colouring dependent on the values.

After choosing the starting line for the HAZ, the width had to be calculated. To calculate the width a reduced strength zone was used.

$$\Delta y_{\text{red}}^{\text{eq}} = \frac{\int_{y_m}^{\infty} (\sigma_b - \sigma) dy}{(\sigma_b - \sigma_{\text{min}})}$$

Equation for reduced strength zone

To find the strength needed the known relationship between hardness and strength in aluminium was used on the average hardness values, $\sigma_{ys} = 3 \cdot \text{HV} - 48,1$. This gave the table below and a reduced strength zone ranging from 3.90 to 4.49. A width of 4mm was approximated for the whole HAZ

$\sigma_b - \sigma \cdot dy$	1	2	3	4	5	6	7	8	9	sum (trapes)	$\Delta y_{\text{eq red}}$
1			92,1	103,1	114,6	99,4	67,9	20,8	-10,6	446,55	3,896596859
0		103	125,2	111,9	110,4	95,1	62	6	0,9	562,55	4,493210863
-1	98,9	121,9	134,1	94,2	78,8	62,2	36,3	-2,6		575,65	4,292692021

Calculations for the reduced strength zone for the different heights in the weld.